Chiroptical Properties of (*R*)-3-Chloro-1-butene and (*R*)-2-Chlorobutane[†]

Mary C. Tam

Department of Chemistry, Virginia Tech, Blacksburg, Virginia 24061

Micah L. Abrams

Department of Chemistry, University of Central Arkansas, Conway, Arkansas 72035

T. Daniel Crawford*

Department of Chemistry, Virginia Tech, Blacksburg, Virginia 24061

Received: January 31, 2007; In Final Form: March 19, 2007

Coupled cluster and density functional models of specific rotation and vacuum UV (VUV) absorption and circular dichroism spectra are reported for the conformationally flexible molecules (*R*)-3-chloro-1-butene and (*R*)-2-chlorobutane. Coupled cluster length- and modified-velocity-gauge representations of the Rosenfeld optical activity tensor yield significantly different specific rotations for (*R*)-3-chloro-1-butene, with the latter providing much closer comparison (within 3%) to the available gas-phase experimental data at 355 and 633 nm. Density functional theory overestimates the experimental rotations for (*R*)-3-chloro-1-butene by approximately 80%. For (*R*)-2-chlorobutane, on the other hand, all three models give reasonable comparison to experiment. The theoretical specific rotations of the individual conformers of (*R*)-3-chloro-1-butene are much larger than those of (*R*)-2-chlorobutane, in disagreement with previous studies of the temperature dependence of the experimental rotations in solution. Simulations of VUV absorption and circular dichroism spectra reveal large differences between the coupled cluster and density functional excitation energies and the rotational strengths. However, while these differences lead to very different specific rotations for (*R*)-3-chloro-1-butene, they have much less impact on the computed specific rotations for (*R*)-2-chlorobutane. In addition, the coupled cluster VUV absorption spectrum of (*R*)-2-chlorobutane compares well to experiment.

I. Introduction

In the past decade, the development of ab initio and density functional models for correctly predicting the optical properties of chiral molecules has proven to be a challenge.[1−4] Although the quantum mechanical underpinnings of optical activity were known as early as 1928 with Rosenfeld's development of the electric-dipole/magnetic-dipole polarizability tensor[5] (the central quantity associated with both optical rotation (OR) and electronic circular dichroism (CD) rotational strengths[6]), more than 50 years passed before the first Hartree−Fock calculations of the Rosenfeld tensor appeared, including the static-limit approximation by Amos[7] and frequency-dependent calculations by Lazzeretti and Zanasi.[8] The first ab initio calculations of CD rotational strengths were reported by Rauk using configuration interaction theory[9] and by Hansen and Bouman using Hartree−Fock theory in the mid-1980s,[10] while the first such calculations of OR were reported by Polavarapu in 1997. Density functional and coupled cluster theory calculations of these properties have appeared much more recently.[11−27]

In two recent studies, Wiberg et al. addressed one of the major obstacles in accurate modeling of optical rotation: conformational flexibility. In a 2003 paper, they examined a series of 3-substituted-1-butenes using density functional theory (DFT).[28] They demonstrated that, although replacing the substituent at the 3-position had little impact, the calculated specific rotation values varied significantly as a function of the dihedral angle of the carbon backbone. For one specific case, (*R*)-3-chloro-1-butene, they reported that the B3LYP specific rotation at 589 nm (the sodium D line) ranged from $[\alpha]_D = +367$ deg dm^{-1} (g/mL)$^{-1}$ at a C═C−C−C dihedral angle of 320° to −526 deg dm^{-1} (g/mL)$^{-1}$ with a dihedral angle of 180°. The final conformationally averaged result of −112 deg dm^{-1} (g/mL)$^{-1}$ (using G2 free energies and B3LYP/6-311++G** rotations) overestimated the (liquid phase) experimental value of −57.3 deg dm^{-1} (g/mL)$^{-1}$ by a factor of 2. In addition, analysis of the temperature dependence of $[\alpha]_D$ in methylcyclohexane, with an assumed free energy difference between the conformers of 1.315 ± 0.025 kcal/mol led to a value of $[\alpha]_D$ for the lowest-energy conformer of -73.5 ± 0.6 deg dm^{-1} (g/mL)$^{-1}$. The average of the rotations for the two higher-energy conformers was found to be $+34.7 \pm 1.5$ deg dm^{-1} (g/mL)$^{-1}$. These results were found to be in sharp contrast to the corresponding B3LYP/6-311++G** values of −188.1 and +104.1 deg dm^{-1} (g/mL)$^{-1}$, respectively. In an effort to reconcile this discrepancy, they also considered the impact of vibrational motion on the calculated rotations. After excluding the torsional motion of the carbon backbone, they reported a room-temperature vibrational correction of +7.95 deg dm^{-1} (g/mL)$^{-1}$, not enough to account for the difference between the experimental and the theoretical optical rotation.

In 2005, Wiberg et al. reported a similar study focusing on the specific rotations of several 2-substituted butanes.[29] For (*R*)-2-chlorobutane, they found that the B3LYP value of $[\alpha]_D$ of −37.1 deg dm^{-1} (g/mL)$^{-1}$ compared well to its experimental

---

[†] Part of the "Thom H. Dunning, Jr., Festschrift".

* Corresponding author. E-mail: crawdad@vt.edu.

10.1021/jp070843d CCC: $37.00

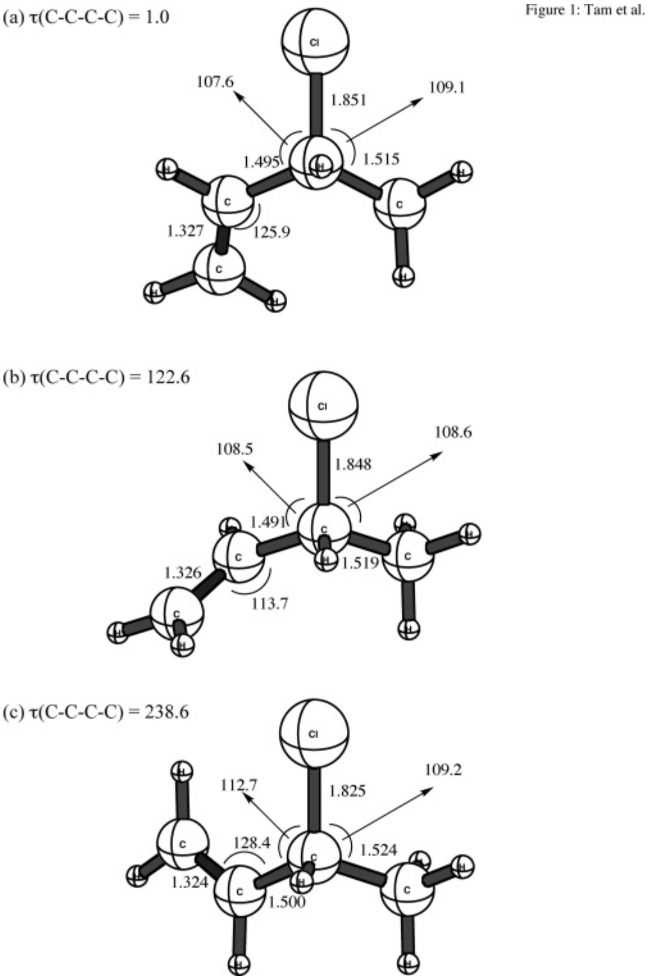

Figure 1. Key parameters of the B3LYP/cc-pVTZ optimized geometries of the three conformers of (*R*)-3-chloro-1-butene, referred to in the text by their C−C−C−C dihedral angles: (a) $\tau \approx 0°$, (b) $\tau \approx 120°$, and (c) $\tau \approx 240°$. Bond lengths are given in Ångstroms, and bond angles are given in degrees.

(neat state) counterpart of −33.8 deg dm^{-1} (g/mL)$^{-1}$, unlike their earlier observations for (*R*)-3-chloro-1-butene. Furthermore, a temperature-dependence analysis similar to that used for (*R*)-3-chloro-1-butene indicated that the lowest-lying conformer of (*R*)-2-chlorobutane exhibited a sodium D-line specific rotation of −77.4 deg dm^{-1} (g/mL)$^{-1}$, while the average of the rotations for the higher-lying conformers was +37.4 deg dm^{-1} (g/mL)$^{-1}$, both very similar to values found for (*R*)-3-chloro-1-butene. They concluded that, even though 3-chloro-1-butene and 2-chlorobutane exhibit very different low-lying electronically excited states, the double bond present in the former has little impact on the measured value of $[\alpha]_D$.

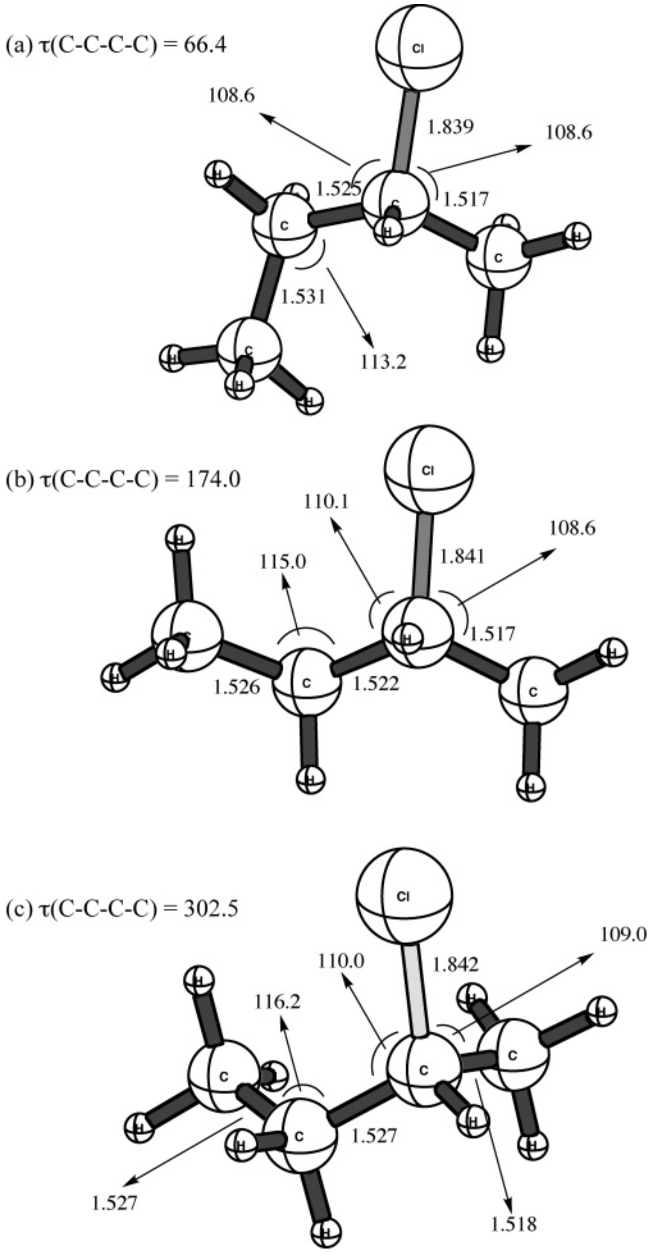

Figure 2. Key parameters of the B3LYP/cc-pVTZ optimized geometries of the three conformers of (*R*)-2-chlorobutane, referred to in the text by their C−C−C−C dihedral angles: (a) $\tau \approx 60°$, (b) $\tau \approx 180°$, and (c) $\tau \approx 300°$. Bond lengths are given in Ångstroms and bond angles are given in degrees.

More recently, Wilson et al. reported[30] experimental specific rotations for both 3-chloro-1-butene and 2-chlorobutane, both in neat liquid and in the gas phase, the latter using the ultrasensitive technique of cavity ring-down polarimetry (CRDP) developed by Vaccaro and co-workers.[31,32] For (*S*)-3-chloro-1-butene, they reported values for $[\alpha]_{633}$ and $[\alpha]_{355}$ of 53.3 ± 1.0 deg dm^{-1} (g/mL)$^{-1}$ and 259.4 ± 1.0 deg dm^{-1} (g/mL)$^{-1}$, respectively, while for (*R*)-2-chlorobutane the comparable values were −32.3 ± 1.0 deg dm^{-1} (g/mL)$^{-1}$ and −121.4 ± 1.2 deg dm^{-1} (g/mL)$^{-1}$. For the neat liquid, they also reported values of $[\alpha]_D$ of 51.6 deg dm^{-1} (g/mL)$^{-1}$ for (*S*)-3-chloro-1-butene and −31.5 deg dm^{-1} (g/mL)$^{-1}$ for (*R*)-2-chlorobutane, in agreement with the earlier results of Wiberg et al.[28,29] Thus, they found only small differences between the gas- and condensed-phase specific rotations for these molecules. However, in agreement with the earlier work, they also found that B3LYP specific rotations agreed well with experiment for 2-chlorobutane, but overestimated those of 3-chloro-1-butene by approximately a factor of 2 (e.g., the B3LYP/aug-cc-pVTZ value of $[\alpha]_{355}$ for (*S*)-3-chloro-1-butene was reported to be 493.7 deg dm^{-1} (g/mL)$^{-1}$).

Previously, we reported theoretical conformationally averaged values of optical rotation for epichlorohydrin using coupled cluster theory and DFT.[27] In comparison to experimental CRDP gas-phase values of $[\alpha]_{355} = -238.7 \pm 2.3$ deg dm^{-1} (g/mL)$^{-1}$ and $[\alpha]_{633} = -55.0 \pm 1.7$ deg dm^{-1} (g/mL)$^{-1}$ for the (*S*) enantiomer published by Wilson et al.,[30] coupled cluster theory (in the singles and doubles approximation, CCSD) yields specific rotations that agree closely with experiment: to within 1% using the length-gauge representation of the electric-dipole operator and within 6% for the modified velocity-gauge representation.[33]

TABLE 1: Specific Rotations (in deg/[dm (g/cm^3)]) of Conformers of (*R*)-3-Chloro-1-butene and (*R*)-2-Chlorobutane at 355 nm[a]

(*R*)-3-Chloro-1-butene

τ	6-311++G(2d,2p)	aug-cc-pVDZ	mixed-cc-pVTZ[b]	aug-cc-pVTZ
B3LYP				
0	1356.2	1330.0	1342.6	1352.3
120	−874.9	−853.2	−862.9	−859.8
240	−485.9	−477.9	−481.6	−484.0
G3	−484.3	−471.9	−477.3	−474.1
CBS CCSD(T)	−476.9	−464.5	−469.9	−466.6
CCSD (Length Gauge)[c]				
0	929.6	933.7	935.3	
120	−649.5	−609.6	−614.9	
240	−230.4	−330.4	−328.3	
G3	−351.0	−337.9	−341.1	
CBS CCSD(T)	−347.5	−332.9	−336.1	
CCSD (Modified Velocity Gauge)				
0	808.2	769.5	783.3	
120	−497.1	−445.2	−453.3	
240	−328.9	−348.6	−346.9	
G3	−277.8	−250.3	−253.6	
CBS CCSD(T)	−272.7	−244.8	−248.1	

(*R*)-2-Chlorobutane

τ	6-311++G(2d,2p)	aug-cc-pVDZ	mixed-cc-pVTZ[b]	aug-cc-pVTZ
B3LYP				
60	48.1	51.6	43.1	46.4
180	−290.8	−284.3	−273.5	−274.4
300	176.5	157.4	167.5	169.0
G3	−145.5	−143.7	−136.8	−136.9
CBS CCSD(T)	−140.3	−138.7	−132.1	−132.0
CCSD (Length Gauge)[c]				
60	25.9	41.6	30.1	
180	−248.1	−222.4	−242.8	
300	148.6	129.1	144.4	
G3	−127.6	−111.2	−124.1	
CBS CCSD(T)	−123.4	−107.2	−119.9	
CCSD (Modified Velocity Gauge)				
60	20.4	41.0	44.7	
180	−234.5	−212.0	−231.2	
300	169.1	124.2	152.2	
G3	−116.9	−105.6	−112.4	
CBS CCSD(T)	−112.8	−101.8	−108.2	

[a] Computed at the B3LYP/cc-pVTZ optimized geometry. [b] aug-cc-pVTZ(C,Cl)+cc-pVDZ(H). [c] Center of mass was used as the coordinate origin.

However, we also found that, while the B3LYP functional produced conformationally averaged rotations that agreed with experiment to within 25%, the rotations of the individual conformers were significantly overestimated relative to CCSD, up to 70% depending on the conformer and wavelength, apparently because of the concomitant underestimation of the excitation energies of low-lying electronic states.

The observations described above beg several questions: Does the double bond of (*R*)-3-chloro-1-butene have any significant impact on the specific rotations of its individual conformers? Why is the B3LYP method apparently able to predict correctly the specific rotation of (*R*)-2-chlorobutane but overestimates the rotation of (*R*)-3-chloro-1-butene by a factor of 2? Can ab initio methods such as coupled cluster theory provide any additional insight into these two paradigmatic systems? This work extends our analysis of conformationally flexible molecules to the problem cases of 3-chloro-1-butene and 2-chlorobutane using coupled cluster methods. We have computed conformationally averaged specific rotations for each molecule at several relevant wavelengths based on high-level estimates of the Gibbs free energies needed to produce accurate gas-phase populations. In addition, we have computed excitation energies, oscillator strengths, and rotational strengths for the four lowest electronic states of each molecule to obtain the first predictions of their conformationally averaged VUV absorption and electronic CD spectra.

II. Computational Details

The Rosenfeld optical activity tensor may be written as[5,6]

$$G'_{\alpha b}(\omega) = -\frac{2}{\hbar}\sum_{n\neq 0}\frac{\omega}{\omega_{n0}^{\;2} - \omega^2}\,\mathrm{Im}\,(\langle 0|\mu_\alpha|n\rangle\,\langle n|\mathrm{m}_\beta|0\rangle) \tag{1}$$

where ω is the frequency of plane-polarized light, μ and m represent the electric and magnetic dipole operators, respectively, and the summation runs over the excited electronic (unperturbed) wave functions. The trace of this tensor is related to the specific rotation of the given conformer, and its residues are related to the rotational strengths of the electronic CD spectrum. We have evaluated G' for 3-chloro-1-butene and 2-chlorobutane at the CCSD level of theory using the linear response formalism of Koch and Jørgensen.[24,34] Two representations of the electric-dipole operator were used with the coupled cluster methods: the standard length-gauge representation, for which the specific rotation is origin dependent, and the velocity gauge, which gives origin-independent results. For the former, the center of mass was chosen as the coordinate origin, and for the latter, we report

TABLE 2: Specific Rotations (in deg/[dm (g/cm^3)]) of Conformers of (*R*)-3-Chloro-1-butene and (*R*)-2-Chlorobutane at 589 nm[a]

(*R*)-3-Chloro-1-butene

τ	6-311++G(2d,2p)	aug-cc-pVDZ	mixed-cc-pVTZ[b]	aug-cc-pVTZ
		B3LYP		
0	316.5	315.2	316.8	319.5
120	−190.5	−189.4	−190.1	−189.1
240	−130.0	−127.0	−128.4	−129.1
G3	−106.0	−105.0	−105.5	−104.5
CBS CCSD(T)	−104.0	−103.0	−103.5	−102.4
		CCSD (Length Gauge)[c]		
0	241.3	245.6	246.1	
120	−165.8	−155.3	−157.0	
240	−85.8	−92.4	−92.3	
G3	−78.3	−86.2	−87.3	
CBS CCSD(T)	−76.5	−84.8	−85.9	
		CCSD (Modified Velocity Gauge)		
0	209.5	199.7	203.9	
120	−122.3	−108.6	−110.8	
240	−91.3	−97.9	−97.9	
G3	−68.4	−61.3	−62.2	
CBS CCSD(T)	−66.9	−59.7	−60.6	

(*R*)-2-Chlorobutane

τ	6-311++G(2d,2p)	aug-cc-pVDZ	mixed-cc-pVTZ[b]	aug-cc-pVTZ
		B3LYP		
60	16.5	17.5	14.9	15.8
180	−90.8	−88.8	−85.0	−85.2
300	58.2	52.2	55.6	55.2
G3	−44.6	−44.1	−41.7	−41.7
CBS CCSD(T)	−43.0	−42.5	−40.2	−40.2
		CCSD (Length Gauge)[c]		
60	9.6	14.6	10.5	
180	−80.0	−70.9	−77.4	
300	49.8	43.2	47.2	
G3	−40.6	−34.9	−39.2	
CBS CCSD(T)	−39.2	−33.6	−37.9	
		CCSD (Modified Velocity Gauge)		
60	7.8	14.3	15.3	
180	−75.8	−67.8	−63.3	
300	57.1	41.9	49.9	
G3	−37.1	−33.2	−28.8	
CBS CCSD(T)	−35.8	−31.9	−27.6	

[a] Computed at the B3LYP/cc-pVTZ optimized geometry. [b] aug-cc-pVTZ(C,Cl)+cc-pVDZ(H). [c] Center of mass was used as the coordinate origin.

the "modified velocity gauge'' approach of Pedersen et al. in which the specific rotation is shifted by its zero-frequency counterpart.[33] In addition, we have computed G' using time-dependent density functional theory with the B3LYP functional.[17,35−37] B3LYP data were obtained using gauge-including atomic orbitals (GIAOs) and are thus origin independent.[17]

For CCSD simulations of VUV absorption and CD spectra, we have computed rotational strengths in the length- and velocity-gauge representations using the equation-of-motion coupled cluster (EOM-CC) formulation for both the excitation energies and the electric-dipole and magnetic-dipole transition moments.[38] For the corresponding B3LYP spectra, we have used the time-dependent formalism.[39−41]

All optical activity calculations reported here made use of the augmented correlation-consistent basis sets of Dunning and co-workers.[42−44] In particular, we have employed the double-ζ and triple-ζ basis sets, denoted aug-cc-pVDZ and aug-cc-pVTZ, respectively, as well as the mixed basis set denoted as "mixed-cc-pVTZ'' that uses the aug-cc-pVTZ basis set for the heavy atoms, carbon and chlorine, and uses the cc-pVDZ basis set for hydrogen.

Structures for each conformer of (*R*)-3-chloro-1-butene and (*R*)-2-chlorobutane were optimized at the B3LYP/cc-pVTZ level of theory. Gibbs free energies were computed using complete basis set (CBS) extrapolations of CCSD(T)/cc-pVDZ and /cc-pVTZ energies along with CCSD(T)/6-31G* corrections for zero-point vibrations and thermal effects (assuming ideal-gas/rigid-rotor models) using the methods described in ref 27. (We note that our earlier work on epichlorohydrin demonstrated that Gibbs free energy differences derived from CBS extrapolations using the DZ/TZ basis-set pair rather than the TZ/QZ pair produced specific rotations that are different by less than 2.0 deg dm^{-1} $(\text{g/mL})^{-1}$ even at short wavelengths.)

All electrons were correlated for the geometry and vibrational frequency calculations, while core electrons (1s for C and Cl) were frozen for single point energies, excitation energies, and CCSD optical rotation calculations (except for the CCSD/mixed-cc-pVTZ optical rotation calculations where the core electrons, 1s for C and 1s2s2p for Cl, were frozen due to memory constraints). Gaussian 03[45] was used for all B3LYP calculations. Coupled cluster structural optimizations and vibrational calculations were carried out with the ACES II package,[46] and all CCSD optical activity calculations were carried out with the PSI3 program package.[47]

TABLE 3: Specific Rotations (in deg/[dm (g/cm^3)]) of Conformers of (*R*)-3-Chloro-1-butene and (*R*)-2-Chlorobutane at 633 nm[a]

(*R*)-3-Chloro-1-butene

τ	6-311++G(2d,2p)	aug-cc-pVDZ	mixed-cc-pVTZ[b]	aug-cc-pVTZ
		B3LYP		
0	265.9	265.1	266.3	268.6
120	−159.1	−158.5	−159.0	−158.1
240	−110.2	−107.6	−108.7	−109.4
G3	−88.6	−87.9	−88.2	−87.4
CBS CCSD(T)	−86.9	−86.2	−86.5	−85.6
		CCSD (Length Gauge)[c]		
0	204.0	207.9	208.3	
120	−140.0	−131.2	−132.6	
240	−72.4	−78.5	−78.4	
G3	−78.6	−72.8	−73.7	
CBS CCSD(T)	−77.6	−71.6	−72.5	
		CCSD (Modified Velocity Gauge)		
0	177.2	168.8	172.5	
120	−103.0	−91.4	−93.3	
240	−77.5	−83.2	−83.2	
G3	−57.6	−51.6	−52.3	
CBS CCSD(T)	−56.3	−50.2	−51.0	

(*R*)-2-Chlorobutane

τ	6-311++G(2d,2p)	aug-cc-pVDZ	mixed-cc-pVTZ[b]	aug-cc-pVTZ
		B3LYP		
60	14.3	15.1	13.6	12.9
180	−77.7	−76.1	−72.9	−72.8
300	50.0	44.9	47.4	47.8
G3	−38.2	−37.7	−35.7	−35.7
CBS CCSD(T)	−36.8	−36.4	−34.3	−34.4
		CCSD (Length Gauge)[c]		
60	8.4	12.6	9.0	
180	−68.0	−60.8	−66.4	
300	42.8	37.1	40.5	
G3	−34.4	−29.9	−33.6	
CBS CCSD(T)	−33.2	−28.8	−32.4	
		CCSD (Modified Velocity Gauge)[c]		
60	6.8	12.3	13.2	
180	−65.0	−58.2	−63.3	
300	49.2	36.0	42.9	
G3	−31.8	−28.4	−30.4	
CBS CCSD(T)	−30.7	−27.4	−29.2	

[a] Computed at the B3LYP/cc-pVTZ optimized geometry. [b] aug-cc-pVTZ(C,Cl)+cc-pVDZ(H). [c] Center of mass was used as the coordinate origin.

III. Results and Discussion

Figures 1 and 2 report the B3LYP/cc-pVTZ optimized structures of (*R*)-3-chloro-1-butene and (*R*)-2-chlorobutane, respectively. In each case, the key parameter is the C−C−C−C dihedral angle (referred to here as τ), along which three minimum-energy structures appear. For 3-chloro-1-butene, the global minimum occurs at $\tau \approx 120°$ with the hydrogen on the stereogenic carbon in the plane of the ethylene unit. Local minima occur at $\tau \approx 0°$ and 240°, approximately 0.9 and 1.4 kcal/mol higher in energy, respectively. For 2-chlorobutane, the global minimum occurs at $\tau \approx 180°$, with local minima at $\tau \approx 60°$ and 300°, approximately 0.6 and 0.9 kcal/mol higher in energy, respectively. These geometries compare well to those of Wiberg et al.[28,29] and were used for all optical activity calculations described below.

A. Optical Rotation. Tables 1, 2, and 3 report the B3LYP and CCSD specific rotations of each conformer of both (*R*)-3-chloro-1-butene and (*R*)-2-chlorobutane, as well as the Boltzmann-averaged results, the latter computed using the populations given in Table 4. We first note that the B3LYP rotations are consistently larger than their CCSD counterparts, a result that is consistant with our earlier findings for monosignant optical rotatory dispersion.[25,27,48] This difference most likely arises from the tendency of the B3LYP approach to underestimate electronic excitation energies (vide infra), leading to small denominators in eq 1.[24]

TABLE 4: Calculated Gas-Phase Conformer Populations

conformation	G3	CBS CCSD(T)
	(*R*)-3-Chloro-1-butene	
0	0.148	0.154
120	0.698	0.705
240	0.154	0.141
	(*R*)-2-Chlorobutane	
60	0.209	0.218
180	0.632	0.618
300	0.159	0.164

More interesting, however, is the relatively large discrepancy between the length-gauge and the modified velocity-gauge CCSD results. For example, the value of $[\alpha]_{355}$ for the $\tau \approx 0°$ conformer of (*R*)-3-chloro-1-butene differs by more than 160 deg dm^{-1} (g/mL)$^{-1}$ for the mixed-cc-pVTZ basis set. This difference is larger than any other system we have studied thus far. Furthermore, the direction of the shifts between the two gauges is not consistent, with the length-gauge approach yielding larger rotations for the $\tau \approx 0°$ and 120° conformers and the

TABLE 5: Excitation Energies (eV), Length-Gauge Oscillator Strengths (Unitless), Length-Gauge and Velocity-Gauge Rotational Strengths (10^{-40} esu^2 cm^2), and $\Delta\langle r^2\rangle$ (in a_0^2) with the aug-cc-pVDZ Basis Set of (*R*)-3-Chloro-1-butene at the B3LYP/cc-pVTZ Optimized Geometry

state	excitation energy	oscillator strength	LG-rotational strength	VG-rotational strength	$\Delta\langle r^2\rangle$	transition
			B3LYP $\tau = 0°$			
1	6.107	0.0400	17.5421	17.2885	6	$n + \pi \rightarrow \pi^* + p$
2	6.139	0.0382	30.0288	29.7003	6	$n + \pi \rightarrow \pi^* + p$
3	6.473	0.0148	35.2844	35.5659	39	$n + \pi \rightarrow p$
4	6.668	0.1890	−1.5243	−0.6686	15	$n + \pi \rightarrow \pi^* + p$
			CCSD $\tau = 0°$			
1	6.879	0.0347	24.5604	18.9077	6	$n \rightarrow p$
2	6.938	0.0204	25.1418	18.2854	6	$n \rightarrow p$
3	7.224	0.0349	31.7432	32.9930	38	$\pi \rightarrow s$
4	7.576	0.3344	−3.3368	−2.3214	14	$\pi \rightarrow p$
			B3LYP $\tau = 120°$			
1	6.148	0.0658	−26.6954	−26.4332	7	$n + \pi \rightarrow \pi^* + p$
2	6.211	0.0102	−12.4695	−12.3334	7	$n \rightarrow \pi^* + p$
3	6.562	0.0294	−28.1990	−28.4624	38	$n + \pi \rightarrow p$
4	6.759	0.2228	−0.7155	−0.9492	19	$n + \pi \rightarrow \pi^* + p$
			CCSD $\tau = 120°$			
1	6.932	0.0556	−30.4025	−21.8527	7	$n \rightarrow p$
2	7.035	0.0039	−8.0203	−7.4587	6	$n \rightarrow p$
3	7.288	0.0329	−20.0985	−19.7789	41	$\pi \rightarrow s$
4	7.648	0.2010	−12.6646	−11.6050	27	$\pi \rightarrow p$
			B3LYP $\tau = 240°$			
1	6.379	0.0369	-0.5199	−0.8945	44	$\pi \rightarrow \pi^* + p$
2	6.660	0.0150	14.3234	14.2207	15	$\pi \rightarrow p$
3	6.850	0.0526	−43.2067	−43.2755	24	$n + \pi \rightarrow \pi^* + p$
4	6.904	0.0137	−3.3672	−3.5716	20	$n \rightarrow \pi^* + p$
			CCSD $\tau = 240°$			
1	7.128	0.0439	4.2683	2.5874	42	$\pi \rightarrow s$
2	7.426	0.0039	−1.6200	−1.8300	9	$n \rightarrow p$
3	7.518	0.0140	2.8561	3.3745	9	$n \rightarrow p$
4	7.726	0.1040	−33.4915	−30.4740	36	$\pi \rightarrow p$

modified velocity gauge yielding a larger rotation for the 240° conformer. For (*R*)-2-chlorobutane, the differences between the two choices of gauge are much smaller.

One measure of the reliability of the length-gauge representation of the optical activity tensor is its origin dependence, which may be computed explicitly via a mixed-gauge polarizability tensor[33] and characterized in terms of the components of an origin-dependence vector. For the aug-cc-pVDZ/CCSD level of theory for (*R*)-3-chloro-1-butene ($\tau \approx 0$), we have computed this vector to be (Δ_x, Δ_y, Δ_z) = (+11.2, −15.9, +26.0) deg dm^{-1} (g/mL)$^{-1}$/a_0 at 589 nm (with the origin placed at the center of mass), with a norm of 32.5 deg dm^{-1} (g/mL)$^{-1}$/a_0, larger than any system we have examined to date. [Even the highly problematic (1*S*, 4*S*)-norbornenone[20] has a maximum vector component of only +6.8 deg dm^{-1} (g/mL)$^{-1}$/a_0 with a norm of 6.8 deg dm^{-1} (g/mL)$^{-1}$/a_0.] The corresponding vector for the $\tau \approx 60°$ conformer of (*R*)-2-chlorobutane is only (Δ_x, Δ_y, Δ_z) = (1.0, 3.6, 1.2) deg dm^{-1} (g/mL)$^{-1}$/a_0 at 589 nm, with a norm of 3.9 deg dm^{-1} (g/mL)$^{-1}$/a_0. This result clearly indicates that the length-gauge data are less reliable than their velocity-gauge counterparts, though it does not necessarily suggest that the origin-dependence is the source of the difference between the two approaches (vide infra).

For (*R*)-3-chloro-1-butene, the modified velocity-gauge results also compare much better to the gas-phase experimental data of Wilson et al.[30] At 355 and 633 nm, the experimental results are +259.4 ± 1.0 and +53.3 ± 1.0 deg dm^{-1} (g/mL)$^{-1}$ (for the *S* enantiomer), as compared to the mixed-cc-pVTZ/CCSD values of $[\alpha]_{355}/[\alpha]_{633} = -253.6/-52.3$ deg dm^{-1} (g/mL)$^{-1}$ and −248.1/−51.0 deg dm^{-1} (g/mL)$^{-1}$ for the G3 and CBS CCSD(T) Boltzmann-averaged values, respectively. The length-gauge approach, on the other hand, yields much larger averaged rotations of −341.1/−73.7 and −336.1/−72.5 deg dm^{-1} (g/mL)$^{-1}$. The B3LYP approach gives −477.3/−88.2 and −469.9/−86.5 deg dm^{-1} (g/mL)$^{-1}$, even further from experiment. For (*R*)-2-chlorobutane, however, all three theoretical models give comparable results, with the length-gauge mixed-cc-pVTZ/CCSD values of −124.1/−33.6 (G3) and −119.9/−32.4 (CBS CCSD(T)) deg dm^{-1} (g/mL)$^{-1}$ slightly closer to the experimental values of $[\alpha]_{355} = -121.4$ deg dm^{-1} (g/mL)$^{-1}$ and $[\alpha]_{633} = -32.3$ deg dm^{-1} (g/mL)$^{-1}$.

Perhaps the most striking result from Tables 1−3 is that the (*R*)-3-chloro-1-butene specific rotations for each of its three conformers are significantly larger in magnitude than those of (*R*)-2-chlorobutane at every level of theory, in disagreement with the findings of Wiberg et al.,[28,29] who reported that the lowest-lying conformer of each molecule ($\tau \approx 120°$ for (*R*)-3-chloro-1-butene and $\tau \approx 180°$ for (*R*)-2-chlorobutane) exhibits similar rotations, based on liquid-phase temperature dependence studies. Furthermore, the sign pattern of the rotations appears to be different from that reported by Wiberg et al. For (*R*)-2-chlorobutane, the lowest-energy conformer at $\tau \approx 180°$ exhibits a negative rotation, while the higher-lying conformers exhibit positive rotations, but for (*R*)-3-chloro-1-butene, the $\tau \approx 0°$ conformer gives a positive rotation, while the two other conformers give negative rotations. In both molecules, however, the conformationally averaged final rotation is negative.

B. Circular Dichroism. Tables 5 and 6 report the excitation energies, oscillator strengths (length gauge), rotational strengths (length and velocity gauges), and shifts in the expectation value of r^2 for the lowest four excited states of each conformer of (*R*)-3-chloro-1-butene and (*R*)-2-chlorobutane, respectively. Figures 3 and 4 are simulations of the corresponding UV/vis and ECD spectra for each conformer. Each of the four excited states reported here are dominated by single-excitations, suggesting that the EOM-CCSD data should be reliable to within

TABLE 6: Excitation Energies (eV), Length-Gauge Oscillator Strengths (Unitless), Length-Gauge and Velocity-Gauge Rotational Strengths (10^{-40} esu^2 cm^2), and $\Delta\langle r^2\rangle$ (in a_0^2) with the aug-cc-pVDZ Basis Set of (*R*)-2-Chlorobutane at the B3LYP/cc-pVTZ Optimized Geometry

state	excitation energy	oscillator strength	LG-rotational strength	VG-rotational strength	$\Delta\langle r^2\rangle$	transition
			B3LYP $\tau = 180°$			
1	6.924	0.0011	−2.0150	−2.0297	9	n → p
2	6.956	0.0005	2.4572	2.5395	10	n → p
3	6.988	0.0211	−3.1206	−2.9882	47	n → s
4	7.012	0.0231	0.7049	0.6681	47	n → s
			CCSD $\tau = 180°$			
1	7.377	0.0030	−0.3705	−0.5038	7	n → p
2	7.408	0.0032	−0.0124	0.3946	7	n → p
3	7.865	0.0327	−2.5106	−2.8226	35	n → p
4	7.884	0.0404	−0.2878	−0.1249	36	n → p
			B3LYP $\tau = 300°$			
1	6.886	0.0147	−8.8405	−8.8027	46	n → s
2	6.913	0.0028	−5.7124	−5.8702	11	n → p
3	6.932	0.0230	9.1371	9.1005	46	n → s
4	6.975	0.0031	1.7735	1.7964	10	n → p
			CCSD $\tau = 300°$			
1	7.367	0.0030	−1.4771	−1.9832	7	n → p
2	7.426	0.0042	1.8300	2.1486	7	n → p
3	7.759	0.0244	−6.3695	−6.1585	36	n → p
4	7.816	0.0452	0.7540	0.6287	37	n → p
			B3LYP $\tau = 60°$			
1	6.782	0.0003	−0.6103	−0.6114	21	n → s
2	6.821	0.0034	3.3471	3.3664	20	n → s
3	7.102	0.0136	2.8580	2.8449	34	n → sp
4	7.138	0.0293	−3.1822	−3.0741	34	n → sp
			CCSD $\tau = 60°$			
1	7.348	0.0009	0.3810	1.3943	7	n → p
2	7.378	0.0012	−0.3353	−1.4455	7	n → p
3	7.852	0.0338	8.1547	8.0576	33	n → sp
4	7.892	0.0493	−7.8874	−7.6694	33	n → sp

approximately 0.2 eV. These results were obtained using the aug-cc-pVDZ basis set. Calibrations using larger basis sets appear to shift the EOM-CCSD excitation energies down by less than 0.05 eV and appear to shift the rotational strengths by less than 1.5 10^{-40} esu^2 cm^2 in most cases.

For (*R*)-3-chloro-1-butene, two of the four EOM-CCSD states originate from lone-pair orbitals on Cl atom and the other two from the π bonding molecular orbital of the ethylene unit. In all four states, the excitation occurs into diffuse Rydberg-type orbitals of s- or p-type character. For the B3LYP approach, the nature of the states is much more mixed, with significant π character appearing in all four transitions. The spectrum of (*R*)-3-chloro-1-butene varies somewhat for each conformer, primarily in the ordering of the states. For the $\tau \approx 0°$ and $\tau \approx 120°$ conformers, the excitation energies and oscillator strengths are very similar, while the rotational strengths for three of the four states change sign between the conformers. This is reasonable because the orientation of the C—Cl bond relative to the C=C—C plane is reversed as τ varies from 0 to 120°. The ordering of the states changes for the $\tau \approx 240°$ conformer, with the $\pi \rightarrow$ s-type Rydberg excitation, which is the third excitation for the 0 and 120° conformers, moving to the lowest transition for the 240° conformer. In addition, the two $n \rightarrow$ p transitions, which are lowest for the 0 and 120° conformers, shift upward at 240° by approximately 0.5 eV at the EOM-CCSD/aug-cc-pVDZ level of theory. For the B3LYP approach, the nature of the states is much more mixed, with significant π contributions appearing in all four transitions. It is also interesting that, for the $\tau \approx 0°$ and 120° conformers, the length- and velocity-gauge rotational strengths for the lowest $n \rightarrow$ p transitions vary by approximately 25%, while most of the other transitions exhibit much smaller shifts between the two gauges. (An exception is the second $n \rightarrow$ p transition for the $\tau \approx 0°$ conformer.)

Additional insight into the difference between the two choices of gauge for both the rotational strengths and the specific rotation (discussed above) of (*R*)-3-chloro-1-butene may be gained by considering the large oscillator strength of the $\pi \rightarrow$ p transition of (*R*)-3-chloro-1-butene, which transition dominates the VUV absorption spectrum for all three conformers (cf. Figure 3). The CCSD length-gauge oscillator strength reported in Table 5 for the $\tau \approx 0°$ conformer is 0.3344, while the corresponding velocity-gauge value is 0.2615 (not reported in the table), a difference of 22%, comparable in magnitude to both the difference in specific rotation (17%) and the rotational strength (30%) for this conformer. However, unlike the CD rotational strengths and specific rotations, the oscillator strength is origin independent in both length and velocity representations of the electric dipole moment. Thus, differences between the two representations may be attributable in part to the basis-set representation of the *r* and *p* operators. However, unlike the Hartree−Fock and Kohn−Sham DFT approaches, the CCSD linear response model is not precisely gauge invariant even in the limit of a complete basis set for these properties.[49] Thus, it seems likely that the underlying physical differences between the two choices of gauge can only be determined from a truly gauge-invariant reformulation of the CC response model,[50,51] which is beyond the scope of this article.

For (*R*)-2-chlorobutane, all four excited states originate from lone-pair orbitals on the Cl atom. For the $\tau \approx 180°$ and $\tau \approx 300°$ conformers, all four EOM-CCSD transitions are to the p-type Rydberg orbitals (centered either near the Cl atom or near the C_3−C_4 bond), while in the $\tau \approx 60°$ conformer, two of the virtual states involved mixed s- and p-type character. For B3LYP, two of the states for the $\tau \approx 180°$ and 300° conformers involve transitions to s-type Rydberg orbitals, which are not significant in the EOM-CC states. The ordering of the EOM-

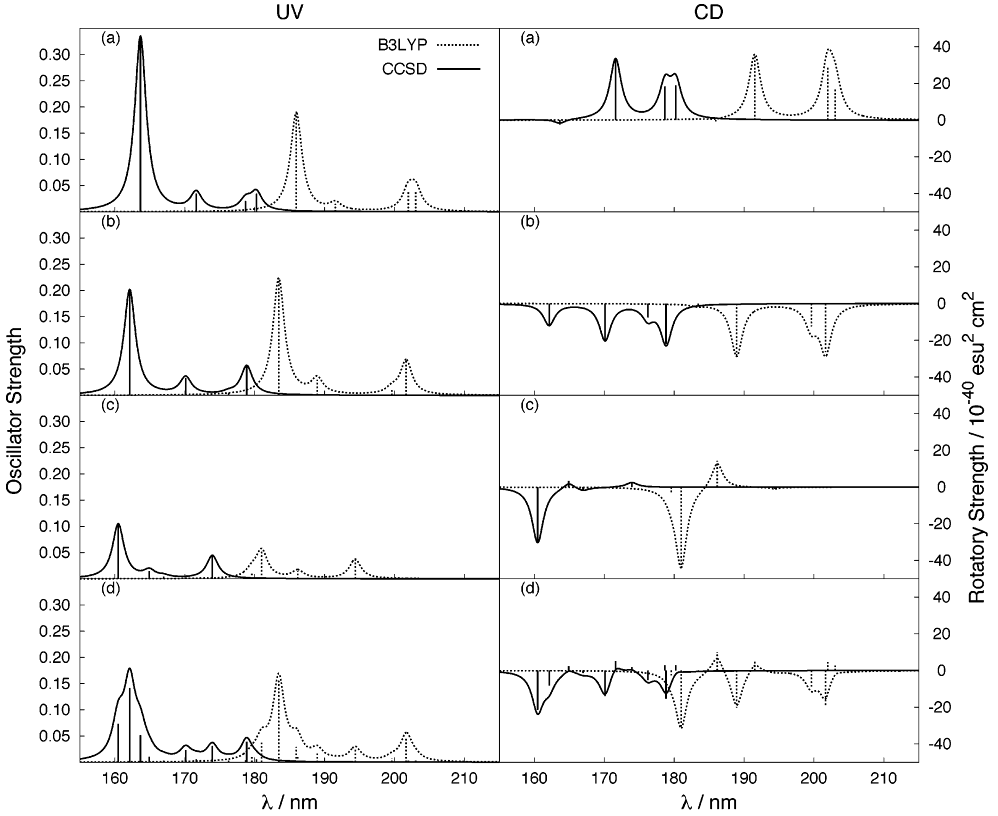

Figure 3. Simulated VUV absorption and CD spectra of (a) 0-conformer, (b) 120-conformer, (c) 240-conformer, and (d) average of the three conformers of (*R*)-3-chloro-1-butene, using vertical excitation energies, oscillator strengths, and rotational strengths from Table 5 and overlapping Lorentzian functions with a full width at half-maximum of 2 nm.

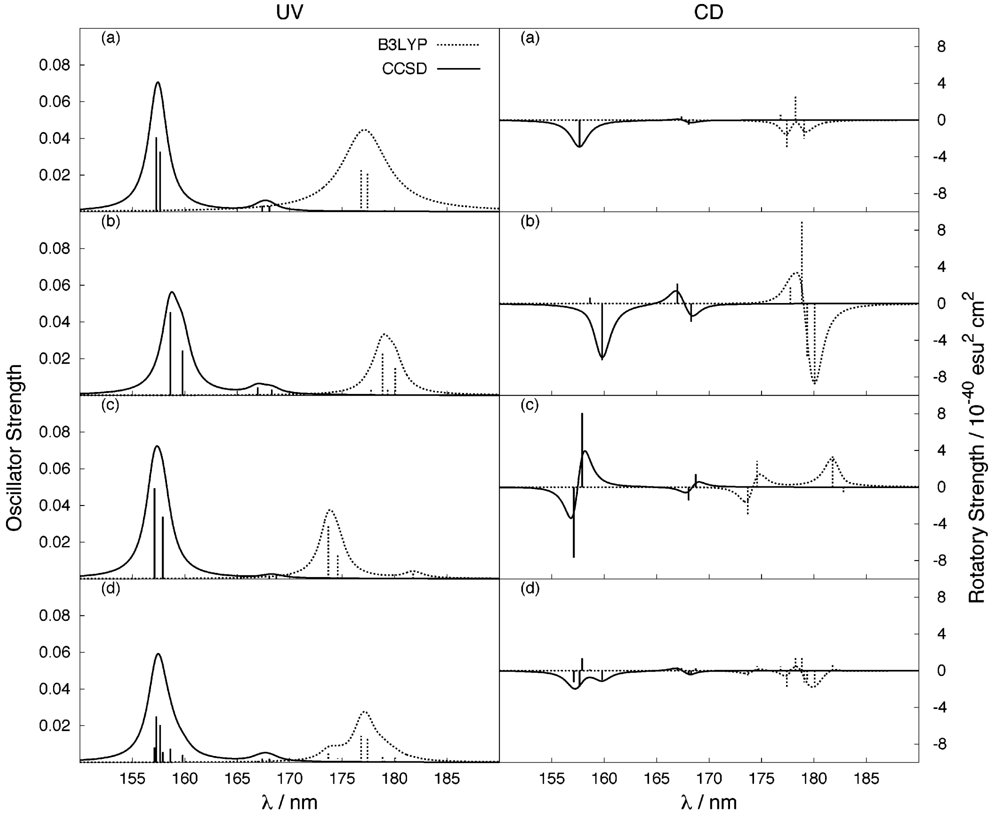

Figure 4. Simulated VUV absorption and CD spectra of (a) 180-conformer, (b) 300-conformer, (c) 60-conformer, and (d) average of the three conformers of (*R*)-2-chlorobutane, using vertical excitation energies, oscillator strengths, and rotational strengths from Table 6 and overlapping Lorentzian functions with a full width at half-maximum of 2 nm.

CCSD states remains unchanged among the conformers, while the rotational strengths change sign as the position of the C−Cl bond relative to the carbon backbone varies, just as that for (*R*)-3-chloro-1-butene.

The simulations in Figures 3 and 4 reveal more clearly the differences between the B3LYP and the CCSD VUV absorption and CD spectra. First, the B3LYP transition energies lie at significantly lower energies than their CCSD counterparts by 0.4 to 0.9 eV (cf. Tables 5 and 6). On the other hand, the shapes of the B3LYP and CCSD spectra for (*R*)-3-chloro-1-butene are similar for all three conformers, with each of the major features reproduced by both models. The spectra for (*R*)-2-chlorobutane, however, differ more substantially, particularly the CD spectra for which the B3LYP and CCSD simulations for the 180° and 300° conformers have little in common. This difference extends to the averaged spectra in Figure 4d, yielding qualitatively different DFT and CC results. In addition, the fact that the larger apparent difference in the B3LYP and CCSD CD spectra do not yield significantly different specific rotations (as discussed in the previous section) is congruous with the recent sum-over-states analysis reported by Wiberg et al. in that the total rotation involves a larger number of electronic states rather than only the lowest few.[52]

Wiberg et al. reported the VUV absorption spectrum of 2-chlorobutane in conjunction with their study of its optical rotation.[29] They found a low-intensity band centered at 57 450 cm^{-1} (7.1 eV, 174 nm) and three stronger bands at 63 310 cm^{-1} (7.8 eV, 158 nm), 67 430 cm^{-1} (8.4 eV, 148 nm), and 72 460 cm^{-1} (9.0 eV, 138 nm). The aug-cc-pVDZ/CCSD simulated absorption spectrum in Figure 4d compares reasonably well with the first two of these bands in both wavelength and intensity (cf. Figure 4 of ref 29), with the weaker band at slightly higher energy. The B3LYP simulation, on the other hand, is shifted to significantly longer wavelengths, and its intensity pattern does not resemble the experimental spectrum.

IV. Conclusions

The recent availability of gas-phase experimental data makes the conformationally flexible molecules (*R*)-3-chloro-1-butene and (*R*)-2-chlorobutane useful test cases for theoretical models of chiroptical properties. For (*R*)-3-chloro-1-butene, the modified velocity-gauge approach with the CCSD method yields Boltzmann-averaged specific rotations that compare closely to the experimental results, while the origin-dependent length-gauge CCSD approach gives rotations that are too large by more than 30%. The discrepancy between the two gauge representations is larger for (*R*)-3-chloro-1-butene than any other system examined to date, and a direct calculation of the origin-dependence vector of the length-gauge model suggests that it is unreliable in this case. B3LYP-based specific rotations are too large by more than 80%, a result that is consistent with our previous study of the conformationally flexible molecule epichlorohydrin.[27] On the other hand, all three models give reasonable rotations for (*R*)-2-chlorobutane, which suggests that the description of electronic excitations from the π orbital of (*R*)-3-chloro-1-butene is more important than previously thought. Simulations of the VUV absorption and electronic CD spectra for the four lowest-lying states of (*R*)-3-chloro-1-butene and (*R*)-2-chlorobutane reveal large discrepancies between CCSD and B3LYP excitation energies and rotational strengths, particularly for the latter molecule. In addition, the shape of the CCSD absorption spectrum for (*R*)-2-chlorobutane compares well to the available experimental spectrum.[29]

Several remaining sources of error must be considered when judging the quality of the theoretical results reported herein. The first is the limited level of electron correlation included in the CCSD approximation. The only system to date for which triple-excitation effects have been reported for optical rotation is (*S*)-methyloxirane.[53] While such effects led to significant shifts in the short wavelength rotation, unlike (*R*)-3-chloro-1-butene and (*R*)-2-chlorobutane, methyloxirane exhibits a small, bisignate ORD that is particularly difficult to model, and the same absolute shifts will not substantially change the comparison with experiment for (*R*)-3-chloro-1-butene and (*R*)-2-chlorobutane.

On the other hand, vibrational motions are much more likely to be significant in this case. As shown recently by Ruud and Zanasi[54] and by Kongsted et al.[53] for methyloxirane, and by Mort and Autschbach for a series of small molecules,[55] zero-point vibrational effects can often be significant, about 20% for conformationally rigid systems. However, as Wiberg et al. noted in 2003,[28] the most significant vibrational contributions for (*R*)-3-chloro-1-butene and (*R*)-2-chlorobutane are likely to arise from the large-amplitude torsional motion of the carbon backbone. This point, however, relates closely to another possible source of error: the use of a simple Boltzmann averaging procedure in which each conformer is considered to be independent of the others. Taking (*R*)-3-chloro-1-butene as an example, we find there is good reason to question the validity of this approximation for two reasons. First, the lowest-energy conformer ($\tau \approx 120°$) lies approximately 0.9 kcal/mol below the next lowest conformer ($\tau \approx 0°$), while the CCSD(T)/6-31G* vibrational frequency of the torsional motions of the carbon backbone is only approximately 100 cm^{-1}. Thus, starting from the zero-point for this vibration, at least three additional vibrational levels in the well for the global minimum will be populated at room temperature before the zero-point level of the next higher conformer. Second, given that the barrier heights between the conformers are relatively small (e.g., only 1.5 kcal/mol between the $\tau \approx 240°$ conformer and the transition state at $\tau \approx 180°$), tunneling effects could lead to mixing of the torsional vibrational wavefunctions. We will report on our efforts to deal with both of these problems, the zero-point vibrational effects and the explicit description of the torsional vibrational mode, in a forthcoming publication.

Acknowledgment. This work was supported by a National Science Foundation CAREER award (CHE-0133174) and a Cottrell Scholar Award from the Research Corporation. The authors are grateful to Prof. Wesley D. Allen (Georgia) for helpful discussions. T.D.C. was supported under subcontract from Oak Ridge National Laboratory by the Scientific Discovery through Advanced Computing (SciDAC) program of the U.S. Department of Energy, the division of Basic Energy Science, Office of Science, under Contract No. DE-AC05-00OR22725 with Oak Ridge National Laboratory.

References and Notes

(1) Stephens, P. J.; McCann, D. M.; Cheeseman, J. R.; Frisch, M. J. *Chirality* **2005**, *17*, S52−S64.

(2) Pecul, M.; Ruud, K. *Adv. Quantum Chem.* **2005**, *50*, 185−212.

(3) Polavarapu, P. L. *Chirality* **2002**, *14*, 768−781.

(4) Crawford, T. D. *Theor. Chem. Acc.* **2006**, *115*, 227−245.

(5) Rosenfeld, L. Z. *Physik* **1928**, *52*, 161.

(6) Caldwell, D. J.; Eyring, H. *The Theory of Optical Activity*; Wiley: New York, 1971.

(7) Amos, R. D. *Chem. Phys. Lett.* **1982**, *87* (1), 23−26.

(8) Lazzeretti, P.; Zanasi, R. *Phys. Rev. A* **1986**, *33* (6), 3727−3741.

(9) Rauk, A. *J. Am. Chem. Soc.* **1984**, *106*, 6517−6524.

(10) Hansen, A. E.; Bouman, T. D. *J. Am. Chem. Soc.* **1985**, *107*, 4828−4839.

(11) Grimme, S. *Chem. Phys. Lett.* **1996**, *259*, 128−137.

(12) Furche, F.; Ahlrichs, R.; Wachsmann, C.; Weber, E.; Sobanski, A.; Vögtle, F.; Grimme, S. *J. Am. Chem. Soc.* **2000**, *122* (8), 1717−1724.

(13) Autschbach, J.; Ziegler, T.; van Gisbergen, S. J. A.; Baerends, E. J. *J. Chem. Phys.* **2002**, *116* (16), 6930−6940.

(14) Autschbach, J.; Jorge, F. E.; Ziegler, T. *Inorg. Chem.* **2003**, *42* (9), 2867−2877.

(15) Pedersen, T. B.; Koch, H.; Ruud, K. *J. Chem. Phys*. **1999**, *110* (6), 2883−2892.

(16) Pedersen, T. B.; Koch, H. *J. Chem. Phys*. **2000**, *112* (5), 2139−2147.

(17) Cheeseman, J. R.; Frisch, M. J.; Devlin, F. J.; Stephens, P. J. *J. Phys. Chem. A* **2000**, *104*, 1039−1046.

(18) Stephens, P. J.; Devlin, F. J.; Cheeseman, J. R.; Frisch, M. J. *J. Phys. Chem. A* **2001**, *105* (22), 5356−5371.

(19) Ruud, K.; Helgaker, T. *Chem. Phys. Lett.* **2002**, *352*, 533−539.

(20) Ruud, K.; Stephens, P. J.; Devlin, F. J.; Taylor, P. R.; Cheeseman, J. R.; Frisch, M. J. *Chem. Phys. Lett*. **2003**, *373*, 606−614.

(21) Goldsmith, M.-R.; Jayasuriya, N.; Beratan, D. N.; Wipf, P. *J. Am. Chem. Soc*. **2003**, *125*, 15696−15697.

(22) Giorgio, E.; Viglione, R. G.; Zanasi, R.; Rosini, C. *J. Am. Chem. Soc*. **2004**, *126*, 12968−12976.

(23) Rinderspacher, B. C.; Schreiner, P. R. *J. Phys. Chem. A* **2004**, *108* (15), 2867−2870.

(24) Tam, M. C.; Russ, N. J.; Crawford, T. D. *J. Chem. Phys.* **2004**, *121*, 3550−3557.

(25) Crawford, T. D.; Owens, L. S.; Tam, M. C.; Schreiner, P. R.; Koch, H. *J. Am. Chem. Soc*. **2005**, *127*, 1368−1369.

(26) Kongsted, J.; Pedersen, T. B.; Strange, M.; Osted, A.; Hansen, A. E.; Mikkelsen, K. V.; Pawlowski, F.; Jørgensen, P.; Hättig, C. *Chem. Phys. Lett*. **2005**, *401*, 385−392.

(27) Tam, M. C.; Crawford, T. D. *J. Phys. Chem. A* **2006**, *110*, 2290−2298.

(28) Wiberg, K. B.; Vaccaro, P. H.; Cheeseman, J. R. *J. Am. Chem. Soc*. **2003**, *125*, 1888−1896.

(29) Wiberg, K. B.; Wang, Y.-G.; Vaccaro, P. H.; Cheeseman, J. R.; Luderer, M. R. *J. Phys. Chem. A* **2005**, *109* (15), 3405−3410.

(30) Wilson, S. M.; Wiberg, K. B.; Cheeseman, J. R.; Frisch, M. J.; Vaccaro, P. H. *J. Phys. Chem. A* **2005**, *109* (51), 11752−11764.

(31) Müller, T.; Wiberg, K. B.; Vaccaro, P. H. *J. Phys. Chem. A* **2000**, *104*, 5959−5968.

(32) Müller, T.; Wiberg, K. B.; Vaccaro, P. H.; Cheeseman, J. R.; Frisch, M. J. *J. Opt. Soc. Am. B* **2002**, *19*, 125−141.

(33) Pedersen, T. B.; Koch, H.; Boman, L.; de Meras, A. M. J. S. *Chem. Phys. Lett.* **2004**, *393* (4−6), 319−326.

(34) Koch, H.; Jørgensen, P. *J. Chem. Phys*. **1990**, *93* (5), 3333−3344.

(35) Becke, A. D. *J. Chem. Phys*. **1993**, *98*, 5648−5652.

(36) Lee, C.; Yang, W.; Parr, R. G. *Phys. Rev. B* **1988**, *37*, 785−789.

(37) Stephens, P. J.; Devlin, F. J. *Chirality* **2000**, *12*, 172−179.

(38) Stanton, J. F.; Bartlett, R. J. *J. Chem. Phys.* **1993**, *98* (9), 7029.

(39) Jamorski, C.; Casida, M. E.; Salahub, D. R. *J. Chem. Phys*. **1996**, *104* (13), 5134−5147.

(40) Bauernschmitt, R.; Ahlrichs, R. *Chem. Phys. Lett*. **1996**, *256* (4−5), 454−464.

(41) Casida, M. E. *Recent Advances in Density Functional Methods;* World Scientific: Singapore, 1995; Vol. 1.

(42) Dunning, T. H. *J. Chem. Phys*. **1989**, *90* (2), 1007.

(43) Kendall, R. A.; Dunning, T. H.; Harrison, R. J. *J. Chem. Phys*. **1992**, *96* (9), 6796−6806.

(44) Woon, D. E.; Dunning, T. H. *J. Chem. Phys*. **1993**, *98* (2), 1358.

(45) Frisch, M. J.; Trucks, G. W.; Schlegel, H. B.; Scuseria, G. E.; Robb, M. A.; Cheeseman, J. R.; Montgomery, J. A., Jr.; Vreven, T.; Kudin, K. N.; Burant, J. C.; Millam, J. M.; Iyengar, S. S.; Tomasi, J.; Barone, V.; Mennucci, B.; Cossi, M.; Scalmani, G.; Rega, N.; Petersson, G. A.; Nakatsuji, H.; Hada, M.; Ehara, M.; Toyota, K.; Fukuda, R.; Hasegawa, J.; Ishida, M.; Nakajima, T.; Honda, Y.; Kitao, O.; Nakai, H.; Klene, M.; Li, X.; Knox, J. E.; Hratchian, H. P.; Cross, J. B.; Bakken, V.; Adamo, C.; Jaramillo, J.; Gomperts, R.; Stratmann, R. E.; Yazyev, O.; Austin, A. J.; Cammi, R.; Pomelli, C.; Ochterski, J. W.; Ayala, P. Y.; Morokuma, K.; Voth, G. A.; Salvador, P.; Dannenberg, J. J.; Zakrzewski, V. G.; Dapprich, S.; Daniels, A. D.; Strain, M. C.; Farkas, O.; Malick, D. K.; Rabuck, A. D.; Raghavachari, K.; Foresman, J. B.; Ortiz, J. V.; Cui, Q.; Baboul, A. G.; Clifford, S.; Cioslowski, J.; Stefanov, B. B.; Liu, G.; Liashenko, A.; Piskorz, P.; Komaromi, I.; Martin, R. L.; Fox, D. J.; Keith, T.; Al-Laham, M. A.; Peng, C. Y.; Nanayakkara, A.; Challacombe, M.; Gill, P. M. W.; Johnson, B.; Chen, W.; Wong, M. W.; Gonzalez, C.; Pople, J. A. *Gaussian 03*, revision C.02; Gaussian, Inc.: Wallingford, CT, 2004.

(46) Stanton, J. F.; Gauss, J.; Watts, J. D.; Lauderdale, W. J.; Bartlett, R. J. *ACES II;* 1993. The package also contains modified versions of the MOLECULE Gaussian integral program of J. Almlöf and P. R. Taylor, the ABACUS integral derivative program written by T. U. Helgaker, 14H. J. Aa. Jensen, P. Jørgensen and P. R. Taylor, and the PROPS property evaluation integral code of P. R. Taylor.

(47) Crawford, T. D.; Sherrill, C. D.; Valeev, E. F.; Fermann, J. T.; King, R. A.; Leininger, M. L.; Brown, S. T.; Janssen, C. L.; Seidl, E. T.; Kenny, J. P.; Allen, W. D. *J. Comp. Chem*. **2007**, in press (doi: 10.1002/jcc.20573).

(48) Kowalczyk, T. D.; Abrams, M. L.; Crawford, T. D. *J. Phys. Chem. A* **2006**, *110*, 7649−7654; submitted.

(49) Pedersen, T. B.; Koch, H. *Chem. Phys. Lett*. **1998**, *293*, 251−260.

(50) Pedersen, T. B.; Koch, H.; Hättig, C. *J. Chem. Phys.* **1999**, *110* (17), 8318−8327.

(51) Pedersen, T. B.; Fernández, B.; Koch, H. *J. Chem. Phys*. **2001**, *114* (16), 6983−6993.

(52) Wibeg, K. B.; Wang, Y.; Wilson, S. M.; Vaccaro, P. H.; Cheeseman, J. R. *J. Phys. Chem. A* **2006**, *110* (51), 13995−14002.

(53) Kongsted, J.; Pedersen, T. B.; Jensen, L.; Hansen, A. E.; Mikkelsen, K. V. *J. Am. Chem. Soc*. **2006**, *128* (3), 976−982.

(54) Ruud, K.; Zanasi, R. *Angew. Chem., Int. Ed.* **2005,** *44* (23), 3594−3596.

(55) Mort, B. C.; Autchsbach, J. *J. Phys. Chem. A* **2005**, *109* (38), 8617−8623.